Journal of Visualization, Vol. 6, No. 4 (2003) 343-352

An Experimental Study on Swirling Flow in a 90 Degree Circular Tube by Using Particle Image Velocimetry

Chang, T. H.*[1] and Lee, H. S.*[2]

*1 Division of Mechanical and Automation Engineering, Kyungnam University, 449 Wolyoung Dong, Masan, Kyungnam, Korea.
*2 Department of Mechanical Engineering, Kyungnam University Graduate School, 449 Wolyoung Dong, Masan, Kyungnam, Korea.

Received 26 January 2003
Revised 28 May 2003

***Abstract*:** The study of swirl flow is of technical and scientific interest because it has an internal recirculation field, and its tangential velocity is related to the curvature of the streamline. The fluid flow for tubes and elbows of heat exchangers has been studied largely through experiments and numerical methods, but studies about swirl flow have been insufficient. Using the Particle Image Velocimetry method, this study found the time averaged velocity distribution, time averaged turbulence intensity with swirl and without swirl flow for Re = 10,000, 15,000, 20,000 and 25,000 along longitudinal sections, and the results appear to be physically reasonable. In addition, streamwise mean velocity distribution was compared with those of Khodadai et al. and Jeong et al.

***Keywords*:** swirl intensity, tangential inlet condition, concave wall, convex wall

1. Introduction

In a bent tube having peculiar geometry with curvature in the flow direction, strong flow occurs three-dimensionally from the entrance of the tube and continues to exist until the exit of the tube. Local flow parameters such as velocity distribution, pressure loss, and the Nusselt number have important meanings in terms of optimization when an engineer designs industrial mechanical devices. In particular, these parameters are very important to the design of heat exchangers in terms of efficient use of energy, with many studies having been conducted on the subject. The first study of internal flows was the work of Thomson (1876) on the bending effect of an internal flow. He theorized on the phenomenon of the interaction between the centrifugal force and the slow motion of fluid in the boundary layer inducing a secondary flow.

Using glass tubes with different degrees of bending, Eustice (1876) conducted experiments over a wide range of Reynolds numbers, involving a large amount of flow visualization work. Based on the experimental results of Eustice, Dean (1928) studied the flow in a bent tube in an interpretive way. Dean also conducted experiments on a fully developed laminar flow from a bent tube with weak bending, and the results were compared with the simple Navier-Stokes formula.

Ito (1959) manufactured bent tubes with a relative radius of Rc = 1.25 ~ 14.6 using brass castings and conducted experiments on the pressure drop of turbulent flows. Through these experiments, results were compared with those of Eustice and Dean and with consideration of

further practical aspects. In addition he presented an experimental formula for the tube friction coefficient from the results of pressure drop experiments.

In the 1960s, Binnie (1962) first employed swirl flows using water in a 90° transparent bent tube and discovered that an air core was generated within the experimental tube.

Using experimental and numerical methods in a 180° bent tube, Rowe (1970) discovered that the secondary flow increases at the beginning of the bend and reaches a peak value before decreasing to the normal state. While conducting an experiment on fluid flow and heat transfer in a 220° square duct, Mori et al. (1971) obtained resistance coefficients and Nusselt numbers in interpretive and experimental ways. Using a swirl generator consisting of a guide vane in a 180° bent tube, Shimizu et al. (1980) conducted a study on hydraulic power loss and velocity distribution using a Pitot tube in water. In a circular 90° bent tube, Sparrow et al. (1986) conducted a mass transfer experiment using naphthalene sublimation in air and a flow visualization experiment using oil lampblack. However, velocity distributions were not measured in these experiments. Khodadadi et al. (1987) obtained results in a numerical-interpretive way at a swirl intensity ($S = 1/R\left[\int_0^r uwr^2 dr / \int_0^r u^2 r dr\right]$) of S = 1.445 and compared these with the work of Murakami et al. (1976) to confirm the consistency of the results. The swirl intensity of S = 1.445 represents a strong swirl flow. It is an area where a negative axial velocity exists, but axial velocity had only a positive velocity distribution. In 1992, Said et al. calculated the local heat transfer coefficient in a 180° bent tube from changes in the color of liquid crystals.

Using hot wire anemometry, Maeng et al. (1991) and Moon et al. (1991) conducted studies on fluid flow and heat transfer in 180° square and rectangular sections, respectively. Lee et al. (1997) conducted an experiment on heat transfer in a 180° bent tube and Chang et al. (2001) obtained the velocity distribution in a horizontal cylindrical tube using particle image velocimetry.

Since the swirl flows have strong three-dimensionality, it is not so easy to get correlative data bundles from the measurement results obtained by point-wise measurement techniques.

We conducted experiments using the two-dimensional particle image velocimetry technique with 21°C water as the fluid. Time averaged velocity distribution and turbulence intensity of the swirl flow generated by a tangential inlet were obtained for a 90° bent tube for Re = 10,000, 15,000, 20,000 and 25,000. The results were compared with those with and without swirl to examine the characteristics of swirl flow in the tube and to contribute to compact and economical design of heat exchanger.

2. Experimental Equipment

Figure 1 shows the experimental setup used in this research. The length, inner diameter and thickness of the test tube are 150 mm, Ø 50 mm and 2 mm, respectively. A glass tube was heated to create a bent tube with a radius of curvature of 190 mm. Component (①) in the figure is a water tank. There is a partition installed inside the water tank that is designed to prevent the water coming from the pump from flowing directly out of the water tank outlet. The water coming out of the water tank goes into a swirl chamber (③) through a hose (②) and then the water is made to flow in a tangential direction by swirl generator (④) before entering the measuring area (⑤). Finally the water goes into a pump (⑥) and is returned to the water tank (①).

As the swirl angle increases, the laser layer or the length of time that particles remain in the measuring area decreases, and therefore an acoustic optical modulator (AOM) that creates light pulses was used. Transparent acrylic tubes of the same inner diameters were installed in the inflow path of the fluid. The velocity of the fluid was regulated by controlling the rotational speed of the water pump and experiments were conducted at Reynolds numbers of 10,000, 15,000, 20,000 and 25,000.

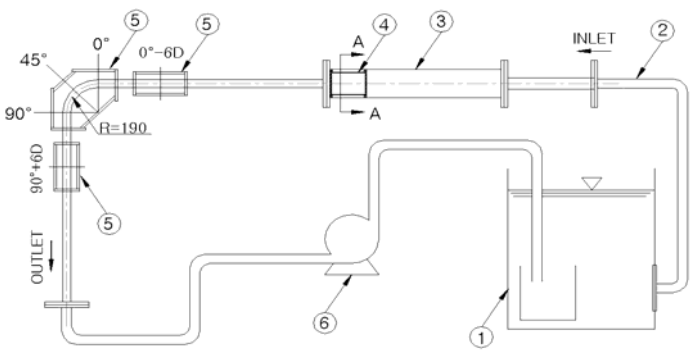

① Water Tank
② Flexible hose
③ Swirl Chamber
④ Swirl Generator
⑤ Test tube ∅ 50 mm
⑥ Water Pump(220V, 3.7kW)

Fig. 1. Schematic diagram of the experimental apparatus.

In non-swirl flow experiments, the swirl generator was removed and a honeycomb was installed at the entrance of the test tube to create the non-swirl flow. The measuring areas were divided into four areas (θ = 0°-6D, θ = 0°, θ = 45° and θ = 90°). Water tanks were installed around each measuring area to prevent light from refracting due to differences in the densities of the fluid and glass tube. In addition, a thin transparent plate was installed on the surface of the water in the water tank to prevent the distortion of images caused by diffuse light reflected from the surface of the water. Figure 2 shows a detailed diagram of a section of the swirl generator. The length and outer diameter of the swirl generator were 218 mm and Ø150 mm respectively and 28 holes of diameter 3 mm were installed in eight groups in the tangential direction. Water enters the swirl generator from the swirl chamber through the four holes located on the outside of the swirl generator and then passes through the Ø3 mm tangential holes to create swirl flow.

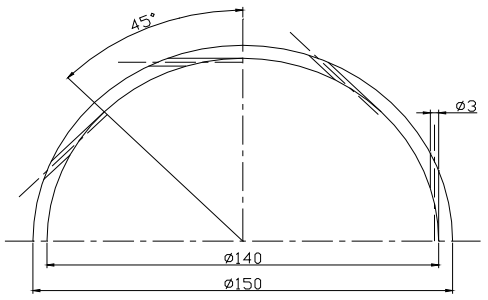

Fig. 2. A-A section views through the swirl generator.

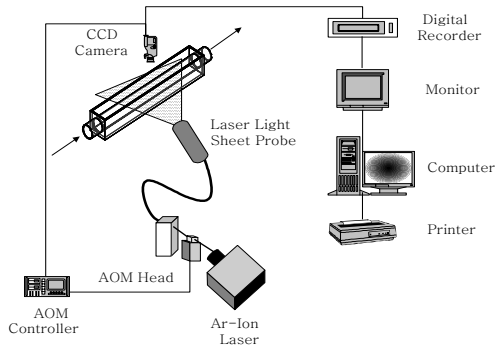

Fig. 3. Schematic arrangement of the PIV system.

3. PIV System

In this study, a 2D-PIV technique was used for swirl and non-swirl flows. An air-cooled 500 mW Ar-ion laser was used as the light source in the experiments. A laser light sheet (LLS) probe, which can move light through optical cable, was used to facilitate the movement of the light source. The LLS can also adjust the thickness of the laser layer by about 1 mm. The length of the optical cable was about 10 m. A Panasonic CCD camera WV3P310, which can capture 30 images per second, was used to obtain flow field data. A digital recorder was used for image recording. Also, a DT3155 (640×480 pixel) board was used to transfer the acquired images to a computer at gray levels ranging from zero to 255. The particles used in the experiment were nylon 12 (120 μm). Figure 3 shows a diagram of the PIV system used in this experiment. For these field images, the velocity vectors were obtained using the PIV algorithm. The calculating time on the host computer (Pentium 550MHz) was

about 3 minutes in the case of the grid 35×70, the radius for the searching area was set to 25 pixels, the size for the correlation area was set to 32×32 pixels. To eliminate erroneous vectors, an error vector elimination method (Hojo et al. 1995) based on the continuous flow condition was adopted.

In order to prohibit the refractive effects of the circular pipe on the results, a square box was installed, which recovered the refracted light waves from the visualized section of the flow.

4. Results and Discussion

4.1 Time Mean Velocity Vector

Figure 4 shows the time mean velocity vector without swirl flow moving along a test tube with a Reynolds number of Re = 10,000. In order to facilitate understanding of the velocity vector profiles, rectangular or band shape boxes with degree scales are employed in Figures 4 and 5, so some areas appear to contain no velocity vectors. Figure 4(a) shows the velocity vector at the front of the inlet of the bent tube at θ = 0°-6D ~ -7D. Figures 4(b) ~ (d) demonstrate the flow changes when the fluid flows from the inlet to the outlet of the bent tube. Figure 4(c) shows the velocity distribution at θ = 45°, which is the central part of the bent tube. In this area, it can be seen that the overlapping of the flow

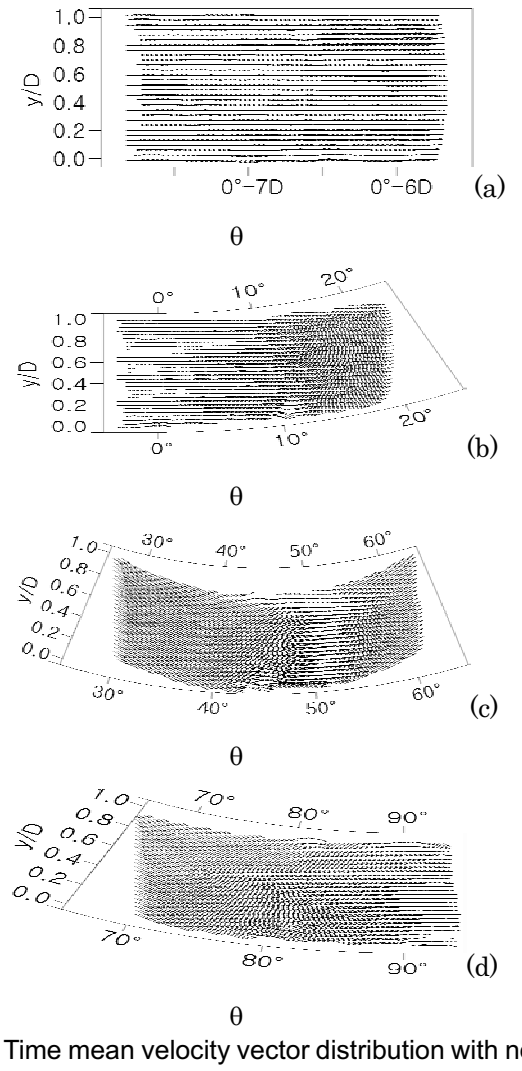

Fig. 4. Time mean velocity vector distribution with non swirl for Re=10,000 at (a) θ=0°-6D, (b) θ= 0° (c) θ=45° and (d) θ=90°.

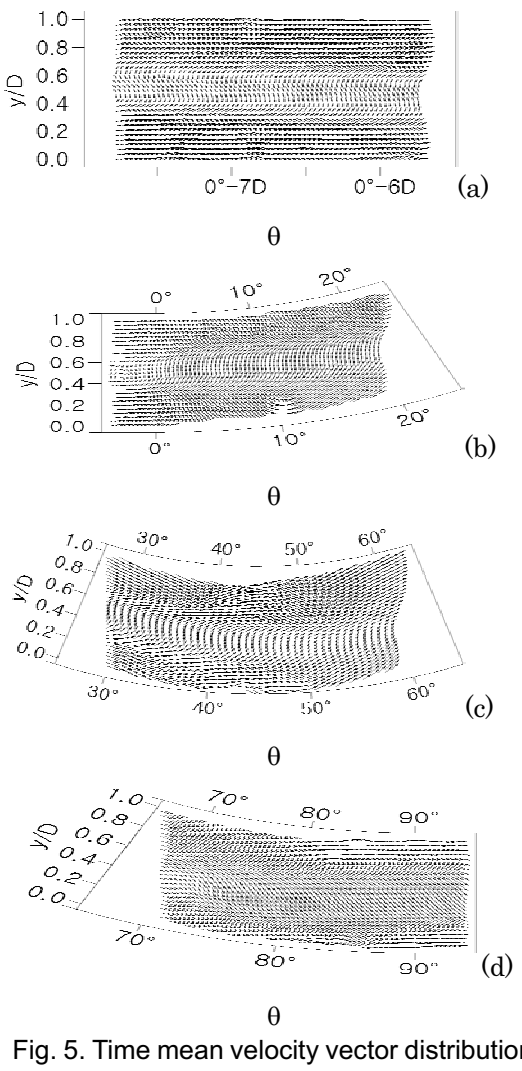

Fig. 5. Time mean velocity vector distribution with swirl for Re=10,000 at (a) θ=0°-6D, (b) θ=0, (c) θ=45° and (d) θ=90°.

occurs at θ = 30° ~ 45° around the concave wall of the test tube, and the secondary flow occurs near the convex wall. The velocity vector shifts toward the concave wall in an even state from θ = 0° to θ = 45°, but moves toward the convex wall beyond that point.

This shows that the flow returns to a turbulent flow distribution state beyond θ= 90°, except around the tube wall area. Figures 5(a) ~ (d) show the velocity vector with swirl flow for Re = 10,000. In Figure 5(a), the straight line at the entrance of the test tube represents the velocity vector at θ= 0°-6D ~ -7D. This shows that a negative velocity vector exists at y/D = 0.4~0.7 in the test tube. Passing through the bent tube, the negative velocity area of the velocity vector component changes in the center of the tube, and the swirl decays near the outlet of the tube. Along the test tube, the velocity vectors area moves toward the outer wall up to θ = 45° and then moves back to the inner wall. The phenomenon of a negative velocity vector at the entrance area of the tube was consistent with the results of Medwell et al. (1989) and Chang et al. (2001) that were conducted with a strong swirl flow in a straight tube.

From the velocity vector, the streamwise mean velocity was obtained for the swirl and non-swirl flows.

4.2 Time Averaged Streamwise Velocity

Figure 6(a) shows the local velocity distribution in a non-swirl flow for Re = 10,000. From the entrance of the test tube, the position of highest velocity moves from the center of the tube to the concave wall. Clearly, from θ = 45° to θ = 90°, the position of highest velocity shifts toward the concave wall. This seems to be caused by centrifugal force due to the influence of the bent tube from the entrance of the test tube. These results remained unchanged, even when the Reynolds number increased, and were consistent with those of the previous studies.

Figures 7(a), (b), (c) and (d) show the local streamwise mean velocity profiles with swirl flow when Re = 10,000, 15,000, 20,000 and 25,000. At the entrance of the test tube, the local velocity shows strong axial velocity near the tube wall and a strong swirl flow demonstrating negative velocity in the center of the tube, much like the velocity vector. Along the test tube, this velocity shifts toward the convex wall until θ = 45° and moves to the concave wall after θ = 45°. In addition the swirl decays and the velocity distribution regains its balance after θ = 90°. This phenomenon was the opposite to the velocity distributions of non-swirl flows in bent tubes that have been reported thus far. This is attributed to the tangential velocity components in the swirl flow and the characteristics of the bent tube.

Figures 8 and 9 show a comparison between the streamwise mean velocity distribution results from the study of Jeong et al. (1996) on a square tube and the results of the studies of Khodadadi et al. (1987) and Murakami et al. (1976) on a circular tube.

In Figure 8, the streamwise velocity distribution was compared with the results of a numerical work by using the "expanded k-ε" turbulence model of Jeong et al. (1996) without swirl flow. When bending was θ = 11.25° and θ = 41.25°, the velocity distribution of Jeong et al. showed a form slightly similar to the data of this study at θ = 90° and when bending was θ = 90°, a slow velocity gradient was demonstrated. But when bending was θ = 0° ~ θ = 45°, there were significant differences. This is attributed to the Re = 750,000 of Jeong et al., which was much higher than Re = 25,000 of this study. In addition, the difference in the equipment may have contributed to the gap. That is, Jeong et al. used a 90° -bent square tube, while this study employed a 90° bent circular tube. However, the velocity distributions showed the same tendency to lean toward the concave wall beyond θ = 45° when Re = 750,000 or Re = 25,000.

However, studies on the swirl flow in a circular tube having a curvature radius are limited. Figure 9 shows a comparison between the analytical results of Khodadadi et al. (1987) and the findings of Murakami et al. (1976) who used a horizontal tube with swirl flow. Both results show Re = 30,000 and demonstrate high velocity near the tube wall and low velocity in the center of the tube. However it looks that these two velocity components were obtained in a weak swirl that does not

demonstrate a negative value. It is especially notable that when X/D = 20, the numerical results of Khodadadi et al. are consistent with the results of the experiment conducted by Murakami et al. Near the center of the tube, however, those results are far different from those of this study. This seems to have been caused by the difference in experimental parameters. For example, although the swirl intensity of Khodadadi et al. was S = 1.445, the velocity decreased near the center at X/D = 5.1, but did not reach negative velocities. This is attributed to the fact that the velocity component obtained in a weak swirl was used as a boundary condition in the numerical interpretation. However, the 2-cell phenomenon of the streamwise velocity distribution was consistent with this work.

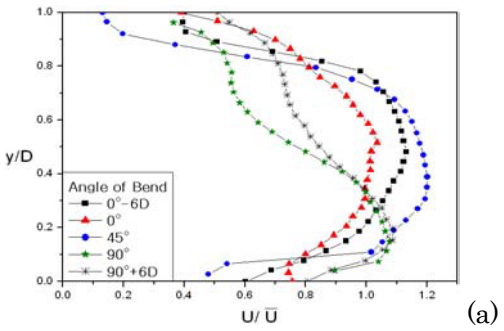

Fig. 6. Streamwise mean velocity profiles with non swirl for (a) Re = 10,000, (b) Re=15,000, (c) Re= 20,000 and (d) Re = 25,000.

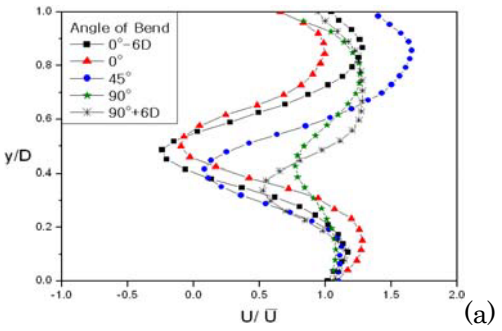

Fig. 7. Streamwise mean velocity profiles with swirl for (a) Re = 10,000, (b) Re=15,000, (c) Re= 20,000 and (d) Re=25,000.

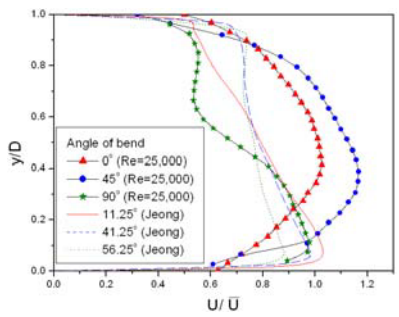

Fig. 8. Comparisons of streamwise mean velocity profiles for non-swirl with result of Jeong.

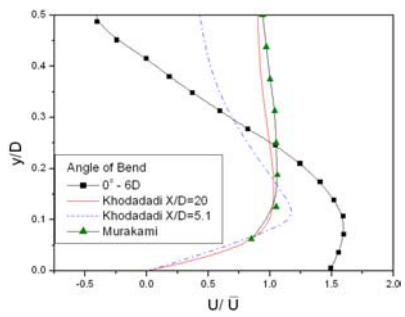

Fig . 9. Comparisons of streamwise mean velocity profiles for swirl with results of Khodadadi and Murakami.

4. 3 Turbulence Intensity

Figure 10 shows the contour of streamwise turbulence intensity without swirl along the test tube for Re = 10,000. Figure 10(c) represents the secondary flow that occurs near the convex wall at θ = 45. Figure 11 includes a contour of turbulence intensity with swirl at (a) θ = 0° - 6D, (b) θ = 0°, (c) θ = 45° and (d) θ = 90° for Re = 10,000.

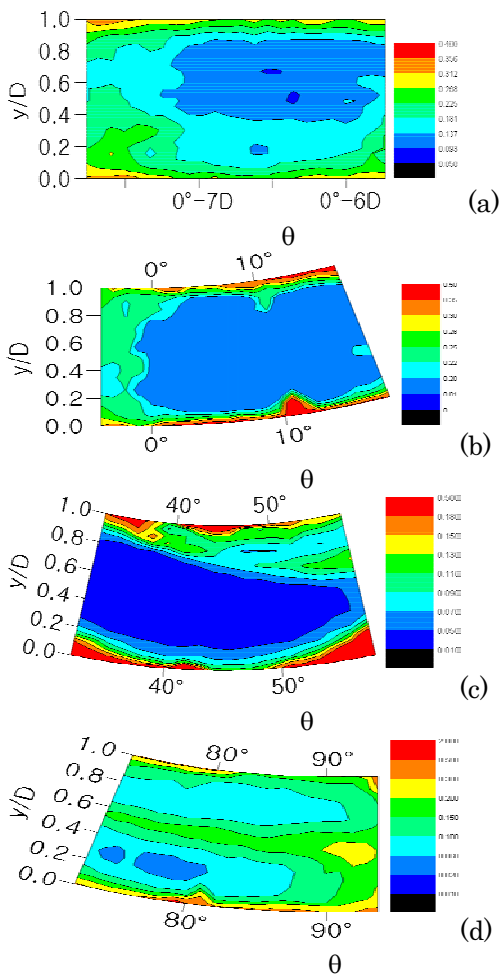

Fig. 10. Contours of streamwise turbulence intensity profiles without swirl for (a) θ=0°-6D, (b) (=0(, (c) (=45(and (d) (=90(for Re=10,000.

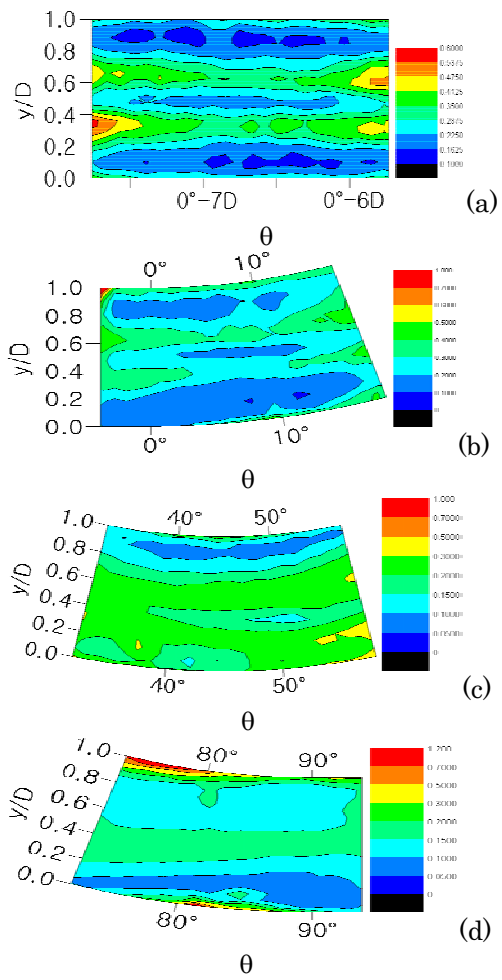

Fig. 11. Contours of streamwise turbulence intensity profiles with swirl for (a) θ=0(-6D, (b) (=0(, (c) (=45(and (d) (=90(for Re=10,000.

Figure 11(a) shows 2-cell phenomenon at y/D = 0.35~0.6 along the test tube and the secondary flow at Figure 11(c) decreased to compare with that of nonswirl flow in Figure 10(c).

Figure 12 shows the local turbulence intensity without swirl for (a) Re = 10,000, (b) Re = 15,000, (c) Re = 20,000 and (d) Re = 25,000 in which the intensity changes along the tube. The maximum turbulence intensity without swirl was observed near the test tube wall, and the value decayed through the tube. At θ = 45°, however, the value was minimized.

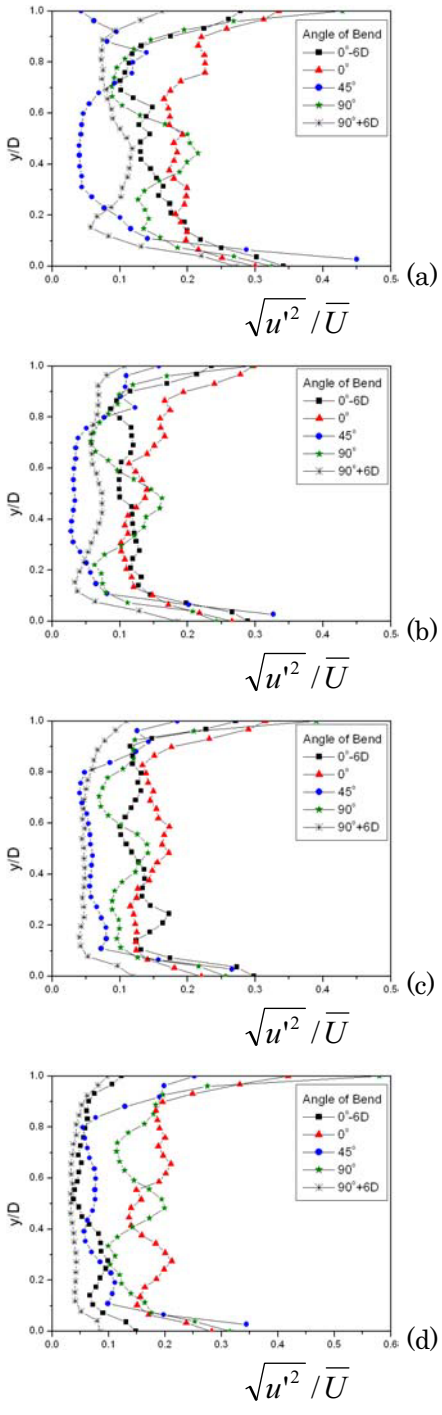

Fig. 12. Time mean turbulence intensity profiles without swirl for (a) Re=10,000, (b) Re=15,000 (c) Re=20,000 and (d) Re=25,000.

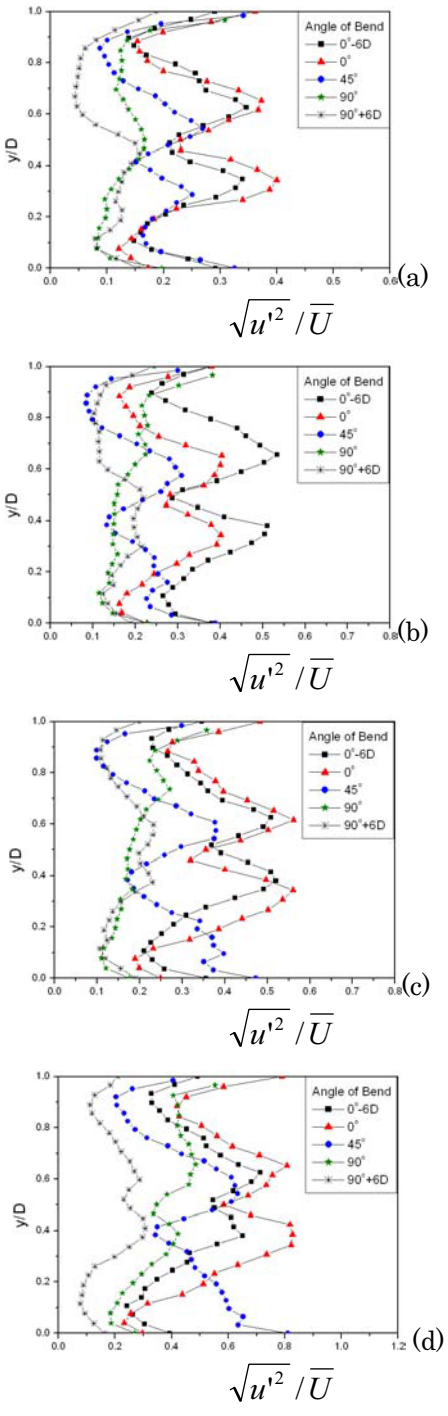

Fig. 13. Time mean turbulence intensity profiles with swirl for (a) Re=10,000, (b) Re=15,000 (c) Re=20,000 and (d) Re=25,000.

The local turbulence intensity with swirl for (a) Re = 10,000, (b) Re = 15,000, (c) Re = 20,000 and (d) Re = 25,000 are included in Figure 13. Figure 13(a) shows the results of calculation of the real time mean turbulence intensity based on the measurements from Figure 11. Like the streamwise mean velocity, the 2-cell phenomenon appears at the entrance of the test tube at θ = 0° -6D ~ -7D. This is attributed to the recirculation zone appearing as a strong swirl flow. That is, when entering the test tube, the maximum zone of turbulent intensity also changes through the 90° bent tube.

As the Reynolds number increased, the two cells continued to exist near θ = 0° for Re = 10,000 and a strong swirl also appeared at θ = 90°+ 6D ~ 7D. It is considered that swirl intensity is a function of the Reynolds number.

According to the results, the 2-cell phenomenon appeared when Re = 10,000 at θ = 0° and when Re = 25,000, the two cells continued to exist until θ = 90°.

The peak of turbulence intensity shifted toward the concave wall from about θ = 45° and as θ increased, the intensity decreased along the test tube. This means that the bent tube has an influence on turbulence intensity. This is attributed to the tangential velocity component of the swirl flow.

5. Conclusion

Using a 2D-PIV technique, this study obtained the time mean velocity distributions and time mean turbulence intensity with swirl and without swirl flow for Reynolds numbers of 10,000, 15,000, 20,000 and 25,000. The authors reached the following conclusions.

1. The peak streamwise velocity of the distribution without swirl flow appeared at y/D = 0.5 and moved along the test tube. From θ = 45°, however, the point shifted to the concave tube wall.
2. In the case of swirl flow, a strong swirl 2-cell phenomenon appeared at the entrance of the tube. The swirl decayed as it moved along the test tube, and the peak streamwise mean velocity zone moved toward the convex tube wall until θ = 45°. Beyond that point, however, the zone shifted toward the concave tube wall.
3. In the case of non-swirl flow, the maximum turbulence intensity showed high values near the tube wall. But in the case of swirl flow, however, a strong 2-cell phenomenon appeared at the entrance of the tube, and the phenomenon diminished as it moved along the test tube together with the decay of swirl intensity. However, when Re = 25,000, a weak 2-cell phenomenon still existed near the exit of the tube.

Acknowledgments

This work is supported by Kyungnam University research fund, 2002.

References

Binnie, A. M., Experimental on the Swirling Flow of Water in a Vertical Pipe and a Bend, Proc. Roy. Soc. A, 270-10 (1962), 452-465.

Chang, T. H. and Kim, H. Y., An Investigation of Swirling Flow in a Cylindrical Tube, KSME Int. J., 15-12 (2001), 1892-1899.

Dean, W., The Streamline Motion of Fluid in a Curved Pipe, Philos Mag, 30 (1928), 673-693.

Eustice, I., Flow of Water in Curved Pipe, Proc. K. Sdc. London Ser. A, 85-1911 (1876), 5-9.

Hojo, K. and Takashima, H., Detection of Erroneous Velocity Vectors Obtained in PIV, J. of Visualization Society of Japan, 15-2 (1995), 177.

Ito, H., Friction Factors for Turbulent Flow in Curved Pipes, J. of Basic Engineering, (1959), 123-134.

Khodadadi, J. M. and Vlachos, N. S., Computation of Confined Swirling Flows: Effects of Boundary Conditions and Turbulence Model, Numerical Method in Laminar and Turbulent Flow, (1987), 458-469.

Jeong, S. J., Kim, T. H. and Cho, J. H., Numerical Computations of Turbulent Flow in a 180°Curved Duct Using a Modified Extended k-Turbulence Model, J. of KSAE, 4-3 (1996), 139-146.

Lee, S. B., Kwon, K. R. and Chang, T. H., A Study on the Heat Transfer Characteristics of Swirling Flow in a Circular Sectioned Bend with Uniform Heat Flux, J. of KSME(B), 21-5 (1997), 615-627.

Maeng, J. S., Lyu, M. S., Yang, S. Y. and Jang, Y. J., Experimental Study of Three Dimensional Turbulent Flow in a 90° Rectangular Cross Sectional Strongly Curved Duct, J. of KSME, 15-1 (1991), 262-273.

Medwell, J. O., Chang, T. H. and Kwon, S. S., A Study of Swirling Flow in a Cylindrical Tube, Korean J. of Air-Conditioning and Refrigeration Engineering, 1 (1989), 265-274.

Moon, C., Lee, G. H. and Choi, Y. D., A Experimental Study on Forced Convective Heat Transfer in a Rectangular Duct with a 180° Bend, J. of KSME, 16-2 (1991), 290-301.
Mori, Y., Uchida, Y. and Ukon, T., Forced Convection Heat Transfer in a Curved Channel with a Square Cross Section, Int. J. of Heat Transfer, 14 (1971), 1787-1805.
Murakami, M., Kito, O., Katayama, Y. and Iida, Y., An Experimental Study of Swirling Flow in Pipes, Bulletin of JSME, 19-128 (1976), 118-126.
Rowe, M., Measurements and Computations of Flow in Pipe Bends, J. Fluid Mech., 43-4 (1970), 771-783.
Said Dini, Nader Saniei and Daniel Bartlett, Use of Liquid Crystal for Local Heat Transfer Coefficient Measurement around a 180 Degree Bend, HTD-Vol. 210, Fundamentals of Convection Heat Transfer ASME, (1992).
Shimizu Yukimaru and Sugino Koichi, Hydraulic Flow Patterns of Swirling Flow in U-Bends, Bulletin E., 23-183 (1980), 1443-1449.
Sparrow, E. M. and Chrysler, G. M., Turbulent Flow and Heat Transfer in Bends of Circular Cross Section : 1-Heat Transfer Experimental, J. of Heat Transfer, 108 (1986), 40-47.
Thomson, J., On the Origin of Winding of River in Alluvial Planic, with Remarks on the Flow of Water Round Bend in Pipe, Proc. K. Sdc. London Ser., 25 (1876), 5-9.

Author Profile

Tae-Hyun Chang : He was educated at Dong-A University(B.E, 1969, M.E. 1971) in Korea. After obtaining his B.E. he was worked at Busan Thermal Power Plant(Korea Electric Company) for 10 years as a mechanical engineer. He obtained his Ph.D. at the department of mechanical engineering of the University of Wales(Swansea, UK) in 1991. He has been working for Kyungnam University since 1978 at the division of mechanical and automation engineering. He was promoted to a professor and appointed the dean of evening school for two years in 1998. He worked as a chairman of ASV'6 at Korea on May 28 – 31 2001. His major research fields are convection heat transfer with and without swirl in a tube. He has published five text books and more than 90 research papers.

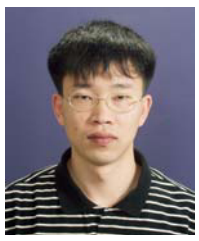

Hae Soo Lee : He received his B.S. degree in Mechanical Engineering from Kyungnam University in 2000 and M.S. degree from the same Institute 2002. His research interest is fluid dynamics using particle image velocimetry.